Supplementary Methods

Animals

All procedures described below have been approved by the Institutional Animal Care and Use Committee of Yale University. Mice were kept under standard laboratory conditions with free access to food (low fat high carbohydrate standard chow) and water. Two sets of *ucp2*$^{-/-}$ mice were used. A gene-trap knockout mouse line was generated by constructs lacking a promoter and including a reporter gene encoding a fusion protein with both β-galactosidase and neomycin phosphotransferase activity, in which the expression of the reporter gene depends on its insertion within an active transcription unit. Introduction of the promoter trap constructs into embryonic stem cells by retroviral infection has led to the derivation of transgenic lines that show a variety of β-galactosidase expression patterns. This method led to a coincidental generation of a *UCP2* knockout line. Another line of *ucp2*$^{-/-}$ mice were provided by Dr Bradford Lowell and have been described elsewhere[28]. G*hsr*$^{-/-}$ mice were obtained from Regeneron Pharmaceuticals Inc (Tarrytown, NY) and bred at Yale University. Characterization of these mice is described elsewhere[3]. NPY-GFP/ *ucp2*$^{-/-}$ and POMC GFP/ *ucp2*$^{-/-}$ mice were produced by crossing NPY-GFP or POMC-GFP mice, as described elsewhere[30] with *ucp2*$^{-/-}$ mice[13]. Mice were backcrossed for at least 6 generations before use to ensure stable genetic background.

Double label Immunohistochemistry for UCP2 and GHSR

Mice were anesthetized and transcardially perfused with 0.9% saline with heparin followed by fixative (4% paraformaldehyde, 15% picric acid, 0.1% glutaraldehyde in 0.1 M PB. Brains were collected and post-fixed overnight before coronal sections were taken at every 50 um. Sections were washed and then treated with 1% H_2O_2 for 15 minutes to remove endogenous peroxidase activity. After washing and blocking with 2% normal horse serum, sections were incubated with primary antibodies. GHSR was immunostained using a rabbit antiserum (1:1000, 4C overnight) raised against the cys portion of the human GHSR sequence (Pheonix Pharmaceuticals Inc). Control sections were incubated antibody preadsorbed with the human GHSR protein (20 mg/ml) or without primary antiserum. UCP2 was observed using *ucp2*$^{-/-}$ mice in which the Lac Z reporter gene was inserted into the promoter of the UCP2 gene. We used mouse anti-beta galactosidase (MP Biomedical, 1:1000 4C overnight) to stain for the Lac Z encoded protein beta

galactosidase. The following day, sections were extensively washed and incubated in fluorescent secondary antibodies (GHSR - donkey anti-rabbit Alexa-fluor 488, UCP2 - donkey anti-mouse alexa fluor 594; all at 1:200 for 60 minutes at RT). Sections were then mounted with VectaShield antifade (Vector Laboratories).

Synaptosomal mitochondrial respiration and membrane potential measurements

UCP2 wt or *ucp2*$^{-/-}$ mice were treated with ghrelin or saline without food available for 1 or 3 hours. The hypothalamus was rapidly dissected and homogenized in the isolation buffer (215 mM mannitol, 75 mM sucrose, 0.1% fatty acid-free BSA, 20 mM HEPES, 1 mM EGTA, pH adjusted to 7.2 with KOH). The homogenate was spun at 1300 x *g* for 3 min, the supernatant was removed, and the pellet was resuspended with isolation buffer and spun again at 1300 x *g* for 3 min. The two sets of supernatants from each sample were topped off with isolation buffer and spun at 13,000 x *g* for 10 min. The supernatant was discarded, and the step was repeated. After this second spin at 13,000 x *g*, the supernatant was discarded, and the pellets were resuspended with isolation buffer without EGTA and spun at 10,000 x *g* for 10 min. The final synaptosomal pellet was resuspended with 50 µl of isolation buffer without EGTA. Heart and muscle mitochondria were isolated as described above except that proteinase was added to the isolation buffer (Nagarase, Sigma USA; 0.4mg/ml). Protein concentrations were determined with a BCA protein assay kit (Pierce, Rockford, IL). Mitochondrial respirations were assessed using a Clark-type oxygen electrode (Hansatech Instruments, Norfolk, UK) at 37°C with pyruvate and malate (5 and 2.5 mM) as oxidative substrates in respiration buffer (215 mM mannitol, 75 mM sucrose, 0.1% fatty acid-free BSA, 20 mM HEPES, 2 mM MgCl, 2.5 mM KH_2PO_4, pH adjusted to 7.2 with KOH). After the addition of oligomycin, UCP-mediated mitochondrial respiration was measured as increased fatty acid-induced respiration[50]. Total uncoupled respiration was also measured after the addition of the photonophore FCCP. For analysis of ADP dependent respiration, ADP was added after the addition of oxidative substrates. The mitochondrial membrane potential was measured in isolated synaptosomal mitochondrial fractions from the hypothalamus using the Δ_m -sensitive TMRE and fluorescent spectrofluorophotometry. Synaptosomal mitochondria (150µg) were incubated in a total volume of 1.5 ml KCl respiration buffer (125 mM KCl, 2 mM $MgCl_2$, 2.5 mM KH_2PO_4, 20 mM HEPES) and 150 nM tetramethylrhodamine ethyl ester perchlorate (TMRE; excitation 550 nm, emission 575 nm) at 37

C and constantly stirred. TMRE is a lipophilic, cationic fluorescent dye that accumulates within mitochondria according to their $\Delta\Psi_m$ in a Nernstian fashion[51, 52] Although, $\Delta\Psi_m$ depolarisation reduces mitochondrial TMRE regardless of the concentration used, TMRE fluorescence of the synaptosomal preparation may either increase or decrease upon Ψ_m depolarisation, depending on the concentration of TMRE used[53]. This is due to the ability of TMRE to self-quench within mitochondria and reduce the fluorescence emanating from the indicator at high concentrations (ie ~150 nM in the synaptosomal preparations of the present study). Under these conditions, mitochondrial TMRE will decrease or cause no change in the fluorescence of individual mitochondria as the $\Delta\Psi_m$ depolarises, but in synaptosomal preparations TMRE fluorescence will transiently increase. TMRE fluorescence does not self-quench within mitochondria at a concentration below ~100 nM and decreases with $\Delta\Psi_m$ depolarization. Thus, as a further control in this study, a sub-quenching concentration of TMRE (10 nM) was also used to monitor the Ψ_m of isolated synaptosomes. Results gained with this sub-quenching dose resulted in mirror traces generated by the 150nM TMRE (data not shown) corresponding to the principles established by Ward et al[53]. Pyruvate (5 mM) and (2.5 mM) malate were added as energy substrates once a baseline reading was achieved. Subsequently, ADP was added (150 μm), followed by oligomycin (1 μm), palmitate (150 μm) and FCCP (1 μm) respectively. Each sample was run in duplicate and the presented data are averaged from each duplicate. Differences in the membrane potential were quantified by assessing relative changes in fluorescence after the addition of substrates, oligomycin and FCCP

Real-time PCR

Mice used in this study were either injected with ghrelin IP (10 nmol) or saline and food was removed. Hypothalami were rapidly collected and snap frozen with liquid nitrogen 3 hours after ghrelin or saline injection. Total RNA was extracted using TRIzol (Invitrogen) following the manufacturer's instructions. cDNA was synthesized by First-Strand cDNA Kit (Amersham Biosciences, Piscataway, NJ) following the manufacturer's instructions. Real-time PCR was performed using SYBR green (Bio Rad laboratories, Hercules, CA, USA) and primers for UCP2 (forward 5'-TCT GGA TAC CGC CAA GGT-3' reverse 5'-TTG TAG AGG CTG CGT GGA-3'), NPY (forward 5'-GCT AGG TAA CAA CGA ATG GGG-3' reverse 5'-CAC ATG GAA GGG TCT TCA AGC-3'), POMC (forward 5'-GGC CCT TCC CCT AGA GTT CA-3' reverse

5'-TTG ATG ATG GCG TTC TTG AA-3'), NRF1 (forward 5'-TGT GCG TTC ATT TGG CTA AG-3' reverse 5'-GTT AAG GGC CAT GGT GAC AG-3'), AgRP (forward 5'-GCA GAC CGA GCA GAA GAA GT-3' reverse 5'-TGC GAC TAC AGA GGT TCG TG-3'), CPT1 (forward 5'-ATG ACG GCT ATG GTG TCT CC-3' reverse 5'-GTG AGG CCA AAC AAG GTG AT-3') and 18S (forward 5'-TTC CGA TAA CGA ACG AGA CTC T-3' reverse 5'-TGG CTG AAC GCC ACT TGT C-3'). Reaction products were confirmed by sequencing of selected samples.

NPY/c-fos staining and stereology

NPY GFP/*ucp2*$^{-/-}$ or POMC GFP/*ucp2*$^{-/-}$ and wt mice were treated with ghrelin or saline and rapidly perfused 1 hour later as described above. NPY and cfos dual immunostaining was performed by sequential addition of primary antibodies. Coronal sections (50 μm) were washed several times and reacted with 1% H_2O_2 in 0.1 M PB solution for 15 minutes. Sections were then washed several times and blocked with 2% normal horse serum and incubated with rabbit anti-cfos (Oncogene) at 1:20,000 at 4^{o}C overnight. Following several washes, sections were incubated with biotinylated donkey anti-rabbit secondary antibody (1:300 1 hr RT), then washed again and incubated in avidin-biotin complex (Vectastain, ABC elite kit, Vector laboratories) for 90 minutes at RT. Immunoreactive cfos was visualized with nickel diaminobenzidine (DAB) reaction for 5 minutes or until desired staining. Sections were then washed extensively and incubated with rabbit anti-GFP (1:5000, 4^{o}C overnight; Molecular Probes, Eugene, Oregon). The following day, sections were extensively washed and incubated with secondary antibody goat anti-rabbit (1:300, 1 hour RT). After washing, sections were incubated in ABC, washed and immunoreactivity was visualized using DAB to reveal a brown precipitation. This approach visualized nuclear cfos as a black precipitate and NPY GFP neurons as brown cytoplasmic staining, allowing for easy identification and quantification of NPY/cfos cells. Sections were then mounted and cover slipped with Depex mounting medium. We then used unbiased stereology methods to quantify NPY/cfos immunoreactive cells in the ARC. Cells were visualized by a Zeiss microscope and relayed via a MicroFibre digital camera (www.optronics.com) to a computer where they were counted using the optical fractionator with the sophisticated StereoInvestigator software (MicroBrightField, Williston, VT, USA). Every fourth section was collected through the ARC nucleus and all NPY, cfos and NPY/cfos cells were counted in grids randomly positioned by the software in the outlined counting area through

all optical planes, thus creating a 3 dimensional counting area. Cells were only counted if they touched the inclusion border or did not touch the exclusion border of the sampling grid.

Electrophysiology

Whole cell recordings were made from NPY GFP/*ucp2*$^{-/-}$ and POMC GFP/ *ucp2*$^{-/-}$ or wt mice. Hypothalamic coronal slices (300 um) containing the ARC were maintained at 33C and perfused with ACSF (NaCl 124 mM; KCl 3 mM, CaCl2 2 mM, MgCl2 2 mM, NaHCO3 26 mM, NaH2PO4 1.23 mM, glucose 3 mM (pH 7.4) with NaOH and was continuously bubbled with 5% CO2 and 95% O2. In the brain section, NPY neurons were patched after a giga ohm seal to observe spontaneous action potential firing. Series resistance was between 20 and 40 Mq and partially compensated by the amplifier. Both input and out resistance and series resistance were monitored throughout the experiments. After the whole cell patch clamp recording was obtained in NPY-GFP neurons, membrane potential and action potentials were recorded under current clamp. To rapidly apply and remove glutamate to (and from) the recorded neurons, a droplet of ACSF containing

glutamate (400 microM) was applied to the bath solution at a distance of about 500 mm away from the recorded neurons. Action potential frequency or miniature post synaptic currents were monitored in control conditions before ghrelin administration, after ghrelin administration (100 nM) and again after ghrelin was washed from the bath solution. The pipette solution contained (mM): Gluconic Acid 140, $CaCl_2$, $MgCl_2$ 2, EGTA 1, HEPES 10, Mg-ATP 4, and Na_2-GTP 0.5, pH 7.3 with KOH. All data were sampled at 3-10 kHz and filtered at 1-3 kHz with an Apple Macintosh computer using Axograph 4.9 (Axon Instruments). Electrophysiological data were analyzed with Axograph 4.9 (Axon Instruments) and plotted with Igor Pro software (WaveMetrics, Lake Oswego, OR, USA). In experiments with FRS, sections were bathed in ACSF containing FRS for 20 minutes before addition of ghrelin. Action potentials were recorded before during and after ghrelin application. Control sections were not incubated in FRS.

Mitochondrial number and quantitative synaptology

Animals were perfused as described above, and their brains were processed for GFP immunolabeling for electron microscopic examination. Ultrathin sections were cut on a Leica ultra microtome, collected on Formvar-coated single-slot grids and analyzed with a Tecnai 12

Biotwin (FEI Company) electron microscope. Mitochondria were counted blindly from randomly selected sections, and Scion Image was used to normalize cytoplasmic area so that mitochondrial density is expressed as number of mitochondria per square micrometers of cytosol. The analysis of synapse number was performed in an unbiased fashion as described elsewhere[3, 30], nonparametric analysis of variance was selected for multiple statistical comparisons. The Mann-Whitney *U*-test was used to determine significance of differences between groups. The statistical confidence was set at P 0.05.

Ghrelin-induced feeding behavior

All mice used in these studies were separated and individually caged two days prior to the start of feeding studies to allow the animals to acclimatize to their new environment. All animals received ghrelin and saline on different days in a cross-over fashion so that the data are reported as the number-fold increase in ghrelin-induced food intake relative to saline levels of food intake. In the evening of the experiment, animals were injected IP with ghrelin (10 nmol) or saline at approximately lights off (7 pm). Food intake was measured at 1, 2 and 3 hours after injection. More than 3 days later, animals that received ghrelin on the first day received saline and those that received saline on the first day received ghrelin. For stereotaxic brain surgery, animals were anesthetized with ketamine (100 mg/ml) and xylazine (20 mg/ml) cocktail. Wild type and *ucp2*$^{-/-}$ mice were implanted with cannulae (Plastics One) into the MBH (A/P -1.8 mm, L 0.15 mm, D/V 5.4 mm + 0.5 mm injector extension) or VTA (A/P -3.3 mm, L 0.25 mm, D/V 4.0 mm + 0.5 mm injector extension). Cannulae were held in place with super glue and dental cement. Mice were allowed to recover for at least 5 days before initiating food intake experiments. Ghrelin was injected in the MBH or VTA (500 pmol/µl) at the beginning of the dark phase and food intake was monitored every hour for three hours post injection. Similar to above, each mouse received both saline and ghrelin injections so that the data are expressed as fold increase in ghrelin-induced food take intake relative to saline. Cannulae placement was verified by histological examination after perfusion. Only those animals showing correct cannula position were included in data analysis.

AICAR treatment

A sterile guide cannula 9 mm in length was implanted into the lateral brain ventricle (0.3 mm posterior and 1 mm lateral relative to bregma, and 3 mm below the surface of the skull). The cannula was then fixed in place using dental cement. After surgery, dummy cannulae were used to prevent blockage. The position of the cannula was verified at the end of the experiments by dye administration before animals were killed. After 5–7 d of postoperative recovery from cannulation, mice were icv injected for over 1 min, with either 2 µl of vehicle (0.9% NaCl) or AICAR (5-Aminoimidazole-4-carboxamide-1-b-D-ribofuranoside; Toronto Research Chemical, North York, Ontario, Canada; 6µg/2 µl). Injections were done immediately preceding dark onset and animals were sacrificed and food intake measured after 3 hours from the beginning of the dark phase. Wild type mice and *ucp2*$^{-/-}$ and ghsr$^{-/-}$ animals were studied (n=5 of each genotype). In order to examine in situ ROS production in identified NPY and POMC neurons we injected DHE (Invitrogen) and ghrelin ip to NPY GFP and POMC GFP wt and *ucp2*$^{-/-}$ mice according to our previous description[26].

Compound C and Etomoxir administration

Immediately prior to peripheral ghrelin injection, *ucp2*$^{-/-}$ and wt mice were injected icv with Compound C (5 µg in 2 µl of vehicle 0.9% NaCl; Sigma, USA) or the CPT1 specific inhibitor etomoxir (1µmol/2 µl of vehicle 0.9% NaCl; Sigma, USA). Food intake was measured over 3 hours after injection (n=5 all groups). In the compound C experiment, data are presented as a percentage increase in food intake measurements after ip saline and icv saline. In the etomoxir experiment, data are expressed as three hour intake in grams. The position of each cannula was verified post mortem at the end of the experiments by dye administration before animals were killed. Only those animals with visible dye in the ventricular system were included in the data analysis.

Measurement of plasma non esterified fatty acids and hypothalamic long chain fatty-acyl CoAs

Nonesterified fatty acids were measured in plasma using a colorimetric nonesterified fatty acid (NEFA) kit (Wako, Richmond, VA), following the manufacturer's instructions. The results were compared with a linear curve using oleic acid as the standard.

Long-chain fatty acyl-CoA (LCFA CoA) standards (C16:0, C16:1, C17:0, C18:0, C18:1, C18:2) were purchased from Sigma (St. Louis, MO). Hypothalami (3 pooled per sample approximately 40-50 mg per sample) were rapidly dissected from mouse brains and frozen in liquid nitrogen until time of assay. LCFA CoAs were extracted by grinding frozen tissue in liquid nitrogen and homogenizing in 1 ml of 100 mM KH2PO4 (pH 4.9) and 1 ml 2-propanol. Heptadecanoyl CoA was added as an internal standard. Saturated (NH4)2SO4 and 2 ml of acetonitrile were added to the suspension and vortexed for 2 min. The emulsion was centrifuged for 10 min at 4,000 rpm, and then the supernatant was diluted with 5 ml of 100 mM KH2PO4 (pH 4.9) for the solid-phase extraction. Before loading, oligonucleotide purification solid-phase columns (Applied Biosystems, Singapore) were conditioned with 5 ml acetonitrile and 2 ml of 25 mM KH2PO4 (pH 4.9). After the samples were loaded, the cartridges were washed with at least 10 ml of distilled water, and then LCFA CoAs were eluted slowly with 0.5 ml of 60% acetonitrile. The eluent was dried in a speed vac and reconstituted in 100 µl of methanol-H2O for electrospray ionization tandem mass spectrometry analysis performed using a bench top tandem mass spectrometer API3000 (Perkin-Elmer Sciex) interfaced with TurboIonspray ionization source. Mobile phase consisted of methanol and H2O with isocratic gradient (50:50). LCFA CoAs were ionized in negative ionspray mode. Doubly charged ions and corresponding product ions were chosen as transition pairs for each CoA species for selective reaction monitoring quantitation. Calibrations of LCFA CoAs showed consistent linearity from 0.2 to 20 ng/µl; coefficiency of variance was 2.1–5.5% for all LCFA CoAs species.

Analyses of ROS production

Wild type and *ucp2*$^{-/-}$ mice were injected with ghrelin (10 nmol) and the hypothalamus was harvested 3 hours later. Synaptosomal mitochondria were isolated as described above. ROS production was quantified using dichlorodihydrofluorescein diacetate (DCF). DCF is a cell permeant indicator for intracellular ROS that is nonfluorescent until the acetate groups are removed by intracellular esterases and oxidation occurs within the cell. Using a fluorescence plate reader (excitation 485 nm, emission 528 nm), hypothalamic ROS in ghrelin-treated or saline-treated samples was estimated in isolated synaptosomes in the presence and absence of oligomycin. Oligomycin induces maximal ROS production as it inhibits the ATP synthase. Data are expressed as arbitrary fluorescence units.

In vivo ghrelin-induced ROS production in identified NPY and POMC GFP neurons in wt or *ucp2*$^{-/-}$ mice was measured by injecting dihydroethidium (DHE) as it is specifically oxidized by superoxide to red fluorescent ethidium. 1 mg/ml was injected into the femoral vein of lightly anathesized mice. Mice were allowed to recover for approximately 90 minutes and were then injected ip with ghrelin (10 nmol) and transcardially perfused 3 hours later. Sections were processed normally for GFP immunohistochemistry. Fluorescent mitochondria (red channel) were counted blindly in NPY or POMC GFP neurons as previously reported [26].

ICV administration of ROS scavenging cocktail

We injected a ROS scavenging cocktail containing ascorbic acid (10 μM), N acetyl-L-cysteine (10 μM) and TEMPO (1 μM) icv to wt or *ucp2*$^{-/-}$ mice with a concurrent ip injection of ghrelin (10 nmol). The ROS scavenging cocktail and ghrelin were administered immediately before the dark phase. Food intake was collected every hour for 3 hours. In a different set of mice, RNA was isolated and PCR performed (as described above) from wt and *ucp2*$^{-/-}$ mice injected with ghrelin or saline ip and the ROS scavenging cocktail or saline icv. The application of this ROS scavenging cocktail also reduced hypothalamic ROS production as measured by DCF and DHE (data not shown).

Statistical Analysis

All data are expressed as the mean ± sem. Data was analysed using the Graph Pad Prism 4.0 program. The means between two groups were analysed by student t-test and between more than two groups and two genotypes by two-way ANOVA followed by Bonferroni posthoc tests unless otherwise stated. Significance was taken at $p<0.05$.

Supplementary figure legends

Supplementary table 1

Genipin decreases mitochondrial respiration but this is neither specific to UCP2 nor uncoupled respiration. Data are presented from brain, heart and muscle mitochondrial respiration in wild type and *ucp2*$^{-/-}$ mice. Data are expressed as the percent decrease in mitochondrial respiration after the addition of genipin. *: $P<0.05$.

Supplementary figure 1

UCP2 and GHSR are colocalized in the arcuate nucleus. **a**: Single channel exposure of beta-galactosidase-immunolabelled positive (representing UCP2) neurons in the ARC. **b**: Single channel exposure of GHSR immunofluorescence (green) in the ARC. **c**: colocalization of GHSR immunoreactivity (green fluorescence) and beta-galactosidase UCP2 labeled (red) in neurons of the ARC. Scale bar on **a** represents 10 μm for panels **a-c**. **d:** Ghrelin increases hypothalamic UCP2 mRNA in a GHSR-dependent manner. **e:** Ghrelin-induced hypothalamic NPY mRNA expression is GHSR-dependent. **f:** Ghrelin-induced hypothalamic AgRP mRNA expression is UCP2-dependent. **g:** Ghrelin had no effect on hypothalamic POMC gene expression. **h**: Ghrelin increases mitochondrial proliferation in UCP2 wt but not *ucp2*$^{-/-}$ mice (**i**). **j:** Ghrelin had no effect on mitochondrial number in POMC neurons. a: Statistically significant differences ($P<0.05$) with respect to saline controls.

Supplementary figure 2

Ghrelin increases mitochondrial number specifically in AgRP-immunoreactive synaptosomes but does not increase total mitochondrial density in isolated synaptosomal pellets. **a**: Mitochondrial density in isolated synaptosomal pellets was determined by counting total mitochondrial number in a known area and the data is expressed as microns squared (μm^2). **b-e**: representative micrographs of hypothalamic synaptosomes in wild type and *ucp2*$^{-/-}$ mice treated with either saline or ghrelin. Note the localization of mitochondria within isolated synaptosomes. **f**: Mitochondrial density in identified immunolabelled AgRP synaptosomes was increased after ghrelin treatment in wt but not *ucp2*$^{-/-}$ mice. **g**: representative images of AgRP-labeled synaptosomes from the hypothalamus of wt and *ucp2*$^{-/-}$ mice. Scale bar equals 1 μm

Supplementary figure 3

a: Ghrelin does not affect mitochondrial membrane potential in hypothalamic synaptosomes from *ucp2*$^{-/-}$ mice.

b-e: UCP2 potentiates NPY cfos activation in the ARC in response to ghrelin (10 nmols). **b**: No c-fos response inwt mice injected with saline and perfused 1 hour later. **c**: NPY-GFP/cfos dual immunohistochemistry of wt mice after ghrelin injection. **d**: NPY-GFP/c-fos dual immunohistochemistry in *ucp2*$^{-/-}$ mice after ghrelin injection. Black arrows on **c** and **d** indicate GFP (NPY) neurons expressing c-fos immunolabeling in response to ghrelin. **e**: Stereological analysis of total NPY-GFP/c-fos cells in the ARC of wt (open bars, n=6) and *ucp2*$^{-/-}$ mice (black bars, n=6). f: Total ARC nucleus volume is not affected by ghrelin treatment or genetic knockout of UCP2. **g:** Ghrelin did not increase c-fos activation in ARC POMC cells and had no affect on total ARC POMC cells or ARC volume (**h&i**).

Supplementary figure 4

a-c: Ghrelin modulates the electrical properties of the hypothalamic melanocortin system in a UCP2 dependent manner. **a**: Representative data showing enhanced action potential firing in wt versus *ucp2*$^{-/-}$ mice in baseline (control), ghrelin and washout conditions. **b:** NPY neurons from *ucp2*$^{-/-}$ mice respond normally to glutamate. Sample traces of glutamate-induced depolarization in NPY neurons from wild type (left) and *ucp2*$^{-/-}$ mice (right) are presented. Arrows indicate application of glutamate to the recorded neurons. RMP: -58.2 mV (left), -76.8 mV (right). **c:** Representative traces showing mIPSCs on POMC-GFP neurons in wt and *ucp2*$^{-/-}$ mice with and without ghrelin application.

d: Ghrelin influences perikaryal synapses of POMC neurons**.** Peripheral ghrelin administration significantly reduces the number of asymmetric, putatively excitatory synapses on POMC neurons 4 hours after injection in wt (saline n = 13, ghrelin n = 18) but not in *ucp2*$^{-/-}$ mice (saline n = 7, ghrelin n = 13). *Ucp2*$^{-/-}$ mice, however, exhibit no reduction of asymmetric putatively excitatory synapse number.

e&f: Low power micrographs showing cannula position in the mediobasal hypothalamus (MBH) or ventral tegmental area (VTA). Note that the asterisk indicates position of the guide cannula and the injection cannula extended 0.5 mm beyond the position of the guide cannula. Scale bar represents 500 microns. **g**: VTA ghrelin injection (500 pmol/µl) significantly increased ghrelin-

induced food intake in both genotypes only at 1 hour post injection. Again, *ucp2*$^{-/-}$ mice displayed attenuated food intake relative to wt controls. The dotted line represents saline food intake. a: statistically significant increase ($P<0.05$) with respect to saline controls. b, Statistically significant reduction ($P<0.05$) with respect to wt mice.

Supplementary figure 5

Lack of UCP2 had no statistically significant effect on the ability of leptin to suppress food intake after an overnight fast although clear trends were observed. a, Food intake (grams) after IP leptin (2 μg) injection (n=4). b, food intake (grams) after mediobasal hypothalamic (MBH) injection of leptin (100 ng/μl, n=5).

Supplementary figure 6

a: Activation of AMPK activity with AICAR significantly enhances mitochondrial respiration and uncoupling activity and this is dependent on the presence of UCP2 as *ucp2*$^{-/-}$ mice do not manifest increases in oxygen consumption in any states of mitochondrial respiration (n = 5). **b&c**: Ghrelin's effect on CPT1, UCP2, NPY and NRF1 occurs rapidly within 1 hour. **d:** Peripheral ghrelin injection increases hypothalamic expression of AgRP mRNA. The expression of both AgRP mRNA however, is completely suppressed by icv injection of etomoxir and CC. Note that mRNA expression was not affected by icv injection of etomoxir or compound C in saline ip injected mice. **e-g**: Ghrelin regulates fatty acid metabolism in the brain and periphery. **e**: Ghrelin increases total hypothalamic pool of long chain fatty acyl CoAs (LCFA CoAs; C 16 and C 18) after 3 hours, n=4-6, three hypothalami pooled per sample, ($p<0.05$). **f**: Time course of LCFA CoA concentration in the hypothalamus after ghrelin injection. **g**: Ghrelin increases nonesterified fatty acids in the plasma of ghrelin injected mice. The results in **f** and **g** show that NEFA rise significantly in the plasma from 60 minutes post ghrelin injection and that LCFA CoAs also peak in the hypothalamus at 60 minutes suggesting that circulating peripheral fatty acids directly contribute to the hypothalamic pool of LCFA CoAs. a: statistically significant ($p<0.05$) with respect to saline mice or time 0 minutes; b: statistically significant ($p<0.05$) with respect to time 30 minutes and c: statistically significant ($p<0.05$) with respect to time 120 minutes.

Supplementary figure 7

Representative images showing in situ putative ROS levels (red fluorescence) after DHE injection in NPY and POMC GFP neurons in wt and *ucp2*$^{-/-}$ mice.

Supplementary figure 8

a: Free radical scavenging (FRS) partially reverses the ghrelin-induced increase in UCP2 mRNA expression (n=5, $p<0.05$). **b:** The FRS cocktail reverses suppressed AgRP mRNA in ghrelin-treated *ucp2*$^{-/-}$ mice. **c:** Incubation of isolated hypothalamic synaptosomes with the FRS cocktail inhibits ghrelin-induced oligomycin-dependent, uncoupled respiration (state 4, n=4, $p<0.05$).

Supplementary figure 9

Schematic diagram showing the proposed sequence of intracellular events leading to ghrelin-induced activation of NPYT/AgRP neurons. Ghrelin binds to its cognate membrane bound receptor (GHSR) on NPY/AgRP neurons leading to immediate induction of action potentials concomitant with phosphorylation and activation of AMPK. Phosphorylation of AMPK inhibits the activity of ACC, reduces malonyl CoA levels and thereby disinhibits CPT1. Increased activity of CPT1 utilizes more LCFA for mitochondrial beta oxidation and subsequently generates ROS production. Fatty acids and ROS increase UCP2-dependent uncoupling activity and UCP2 mRNA, which subsequently reduces overproduction of ROS in a feedback manner, and, thus reduces the inhibitory effect of ROS on CPT1 activity (as indicated by the dashed line with negative symbol) and contributes to the maintenance of increased action potentials. Buffering of ROS production by UCP2 allows appropriate ghrelin-dependent gene transcription events to occur. Increased mitochondrial biogenesis in wt mice enables sustained neuronal firing over time.

Supplementary Table 1

Effect of genipin of mitochondrial respiration

(data expressed as percentage decrease compared to ADP, oligomycin or FFA)

	Brain		Heart		Muscle	
	Ucp2 wt	Ucp2 -/-	Ucp2 wt	Ucp2 -/-	Ucp2 wt	Ucp2 -/-
State 3 Genipin added after ADP	8.1± 0.5*	7.3 ± 0.9*	10.0 ± 1.8*	14.1 ± 2.1*	7.8 ± 0.4*	6.0 ± 0.6*
State 4 Genipin added after oligomycin	13.0 ± 2.0*	9.6 ± 1.3*	7.0 ± 0.5*	5.1 ± 0.7*	8.0 ± 0.5*	12.1 ± 2.7*
FFA Genipin added after palmitate-induced respiration	6.2 ± 0.7*	8.1 ± 1.5*	25.1 ± 3.0*	22.3 ±2.4*	23.4 ± 1.3*	26.8 ± 1.8*

Suppl. Fig. 1

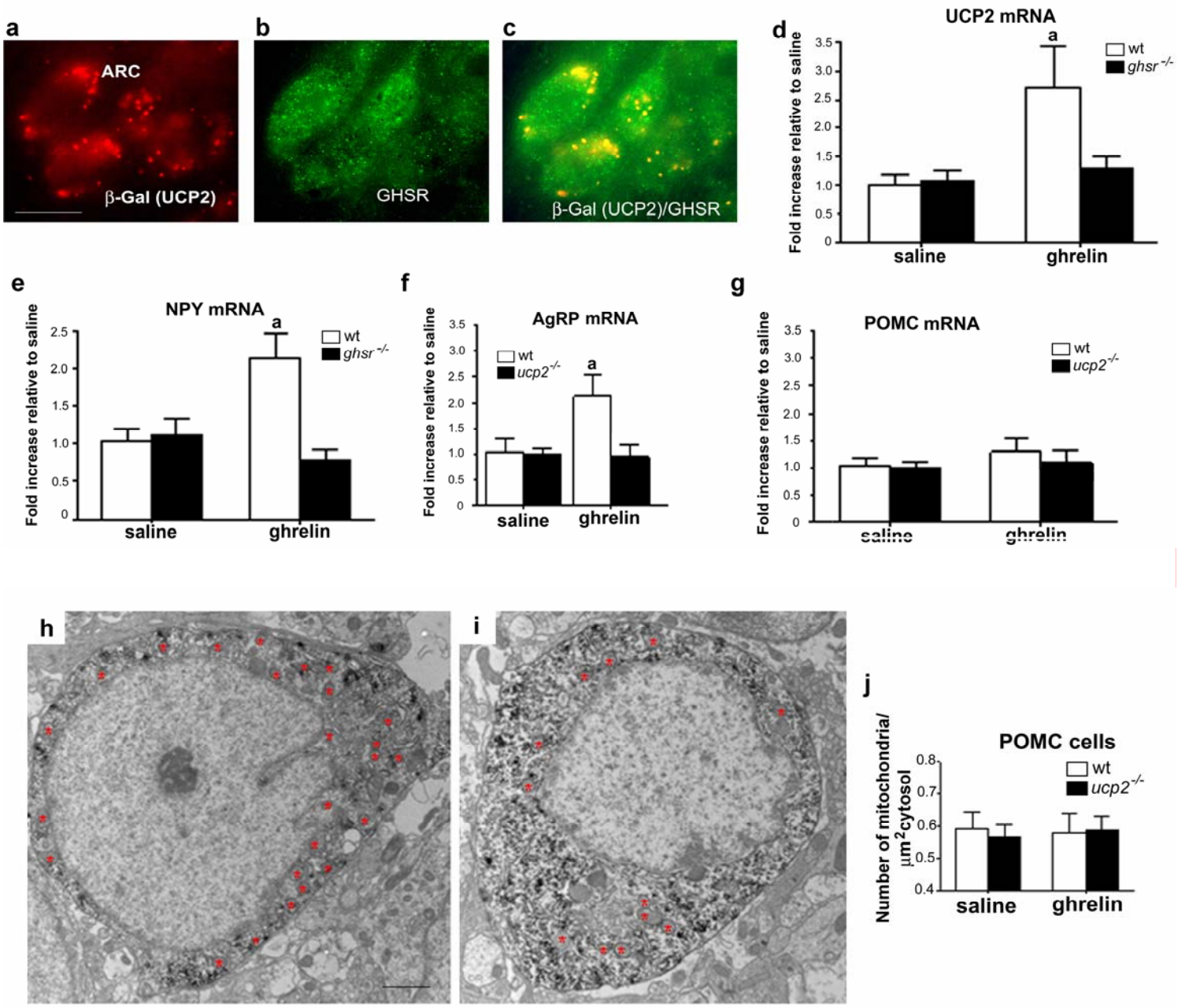
a
ARC
β-Gal (UCP2)
b
GHSR
c
β-Gal (UCP2)/GHSR
d
UCP2 mRNA
Fold increase relative to saline
wt
ghsr -/-
a
saline
ghrelin
e
NPY mRNA
Fold increase relative to saline
wt
ghsr -/-
a
saline
ghrelin
f
AgRP mRNA
Fold increase relative to saline
wt
ucp2-/-
a
saline
ghrelin
g
POMC mRNA
Fold increase relative to saline
wt
ucp2-/-
saline
ghrelin
h
i
j
POMC cells
Number of mitochondria/ µm2cytosol
wt
ucp2-/-
saline
ghrelin

Suppl. Fig. 2

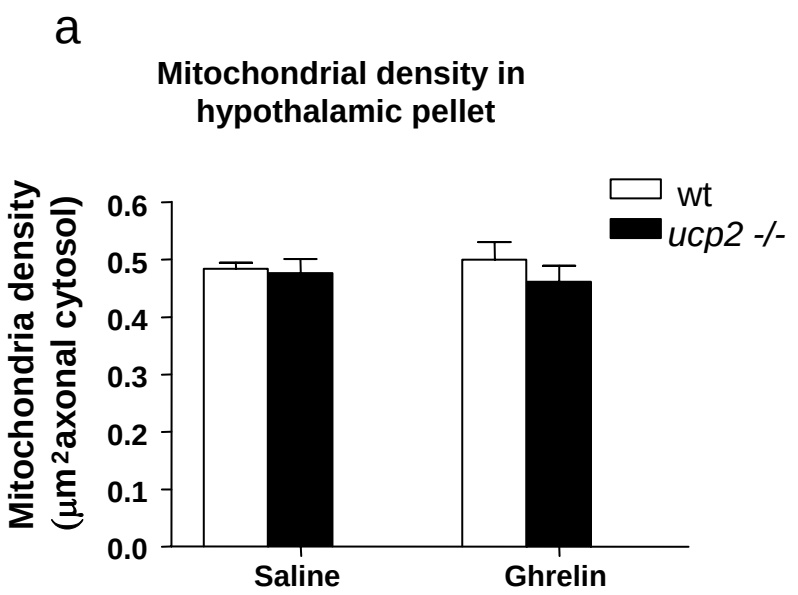
a
Mitochondrial density in hypothalamic pellet
Mitochondria density (μm²axonal cytosol)
0.6
0.5
0.4
0.3
0.2
0.1
0.0
wt
ucp2 -/-
Saline
Ghrelin

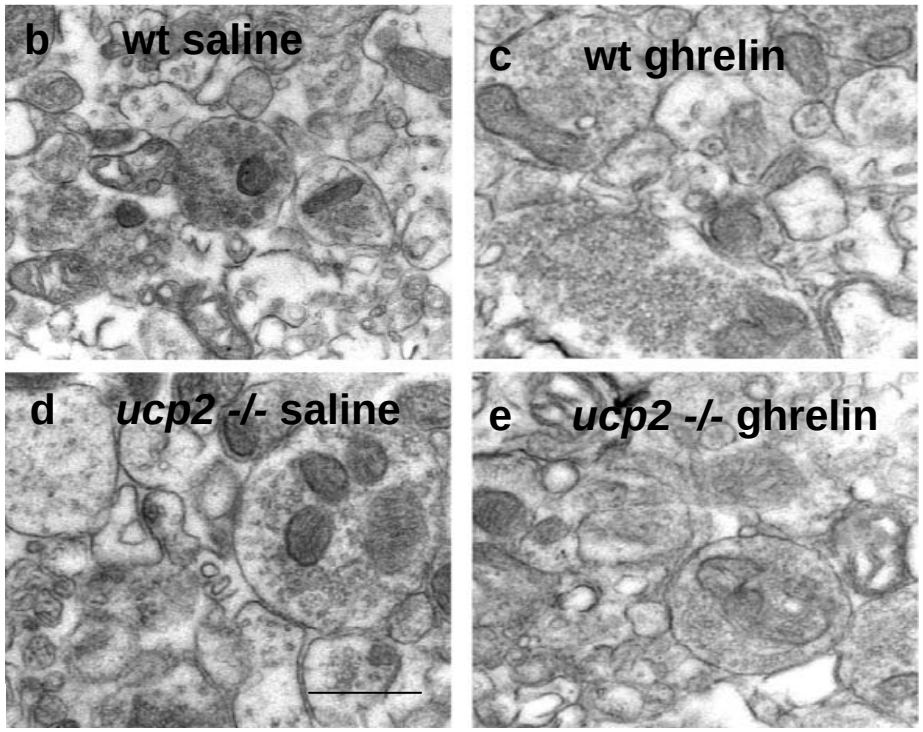
b wt saline
c wt ghrelin
d ucp2 -/- saline
e ucp2 -/- ghrelin

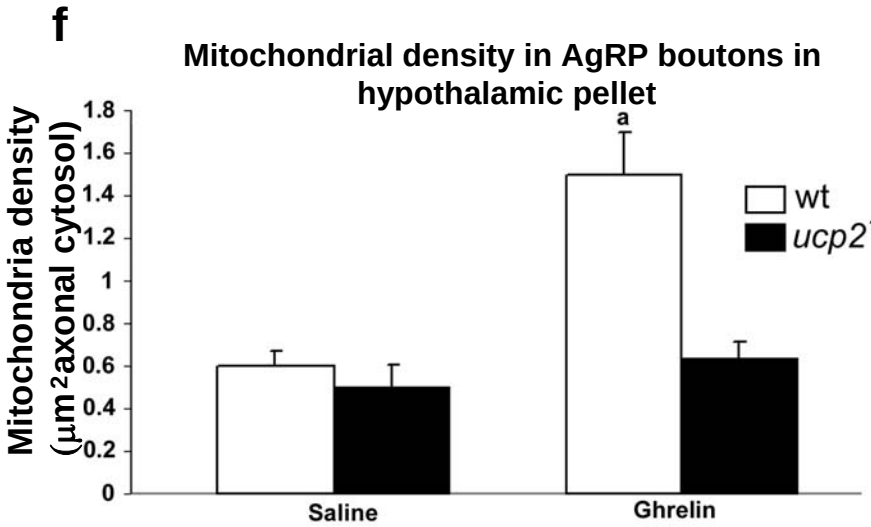
f
Mitochondrial density in AgRP boutons in hypothalamic pellet
Mitochondria density (μm²axonal cytosol)
1.8
1.6
1.4
1.2
1
0.8
0.6
0.4
0.2
0
a
wt
ucp2-/-
Saline
Ghrelin

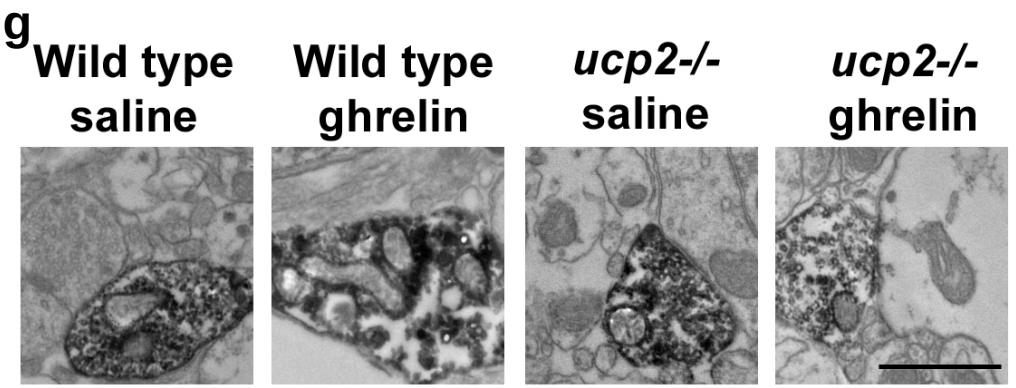
g
Wild type saline
Wild type ghrelin
ucp2-/- saline
ucp2-/- ghrelin

Suppl. Fig. 3

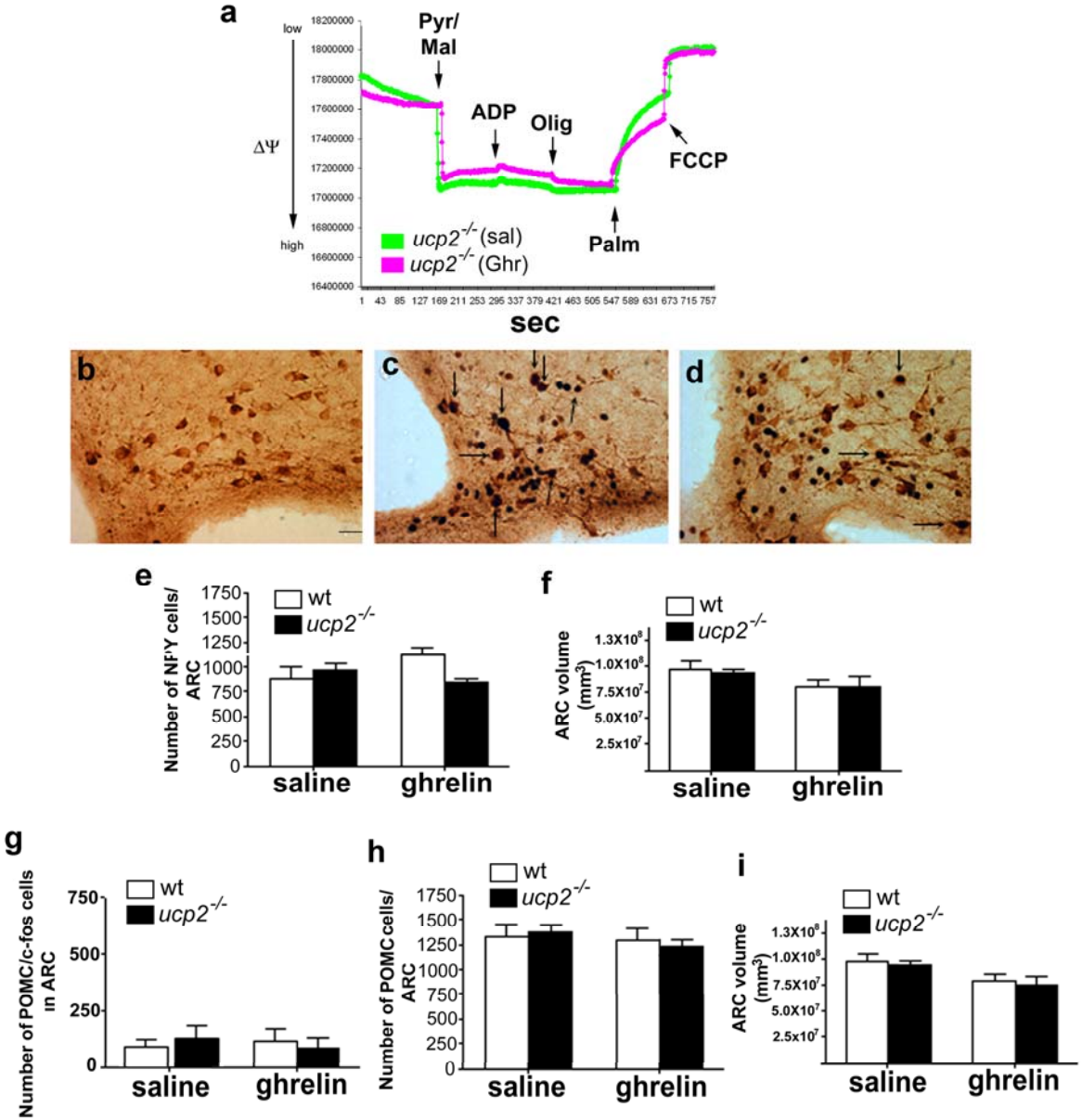
a
low
high
ΔΨ
Pyr/
Mal
ADP
Olig
FCCP
Palm
ucp2-/- (sal)
ucp2-/- (Ghr)
sec
b
c
d
e
Number of NPY cells/ ARC
wt
ucp2-/-
saline
ghrelin
f
ARC volume (mm3)
g
Number of POMC/c-fos cells in ARC
h
Number of POMC cells/ ARC
i

Suppl. Fig. 4

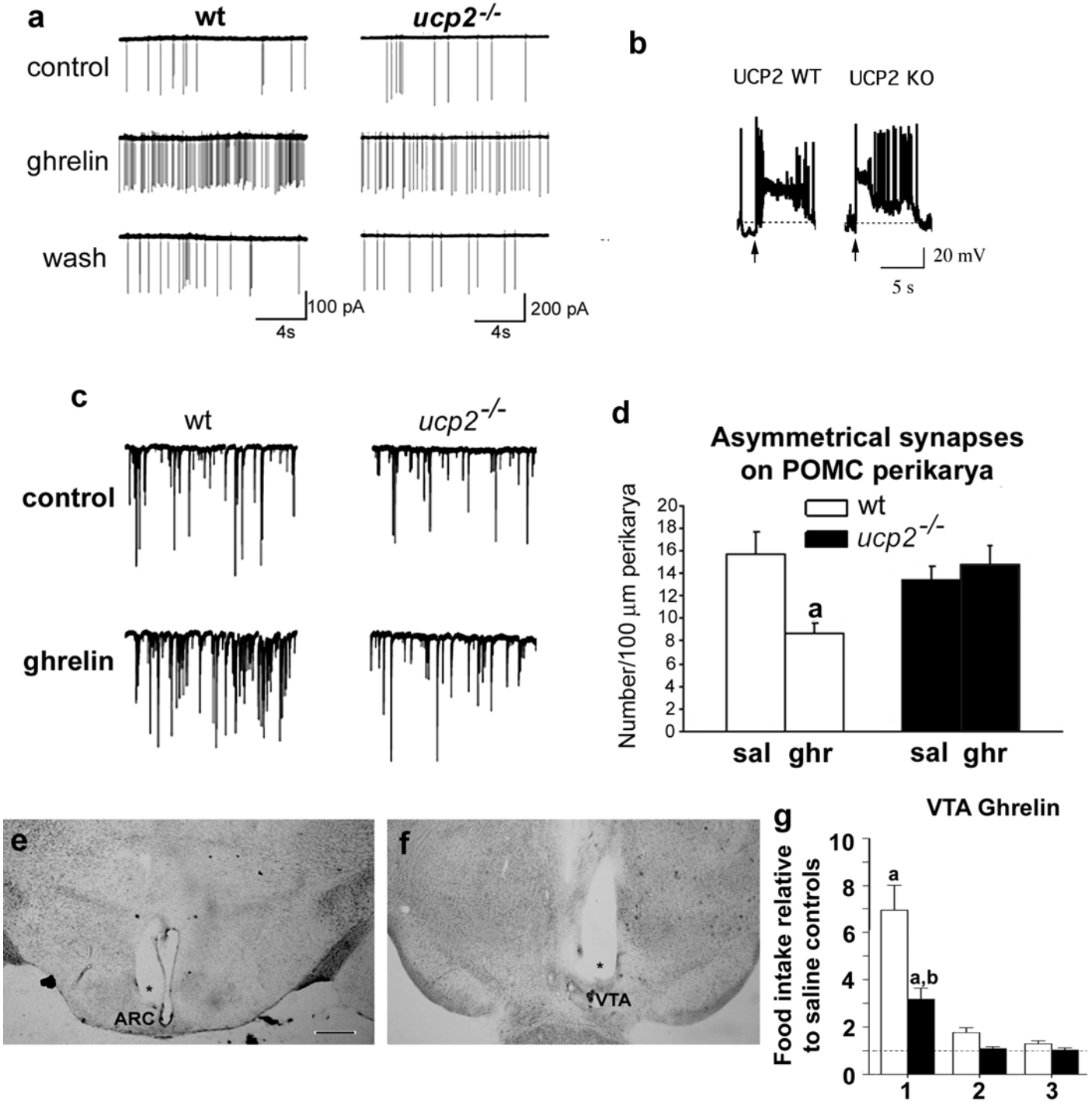
a
wt
ucp2-/-
control
ghrelin
wash
100 pA
4s
200 pA
4s
b
UCP2 WT
UCP2 KO
20 mV
5 s
c
wt
ucp2-/-
control
ghrelin
d
Asymmetrical synapses on POMC perikarya
wt
ucp2-/-
Number/100 µm perikarya
a
sal ghr
sal ghr
e
ARC
f
VTA
g
VTA Ghrelin
Food intake relative to saline controls
a
a,b
1
2
3

Suppl. Fig. 5

Leptin's effect on 4 hour food intake in UCP2 wt mice more than in UCP2 ko mice

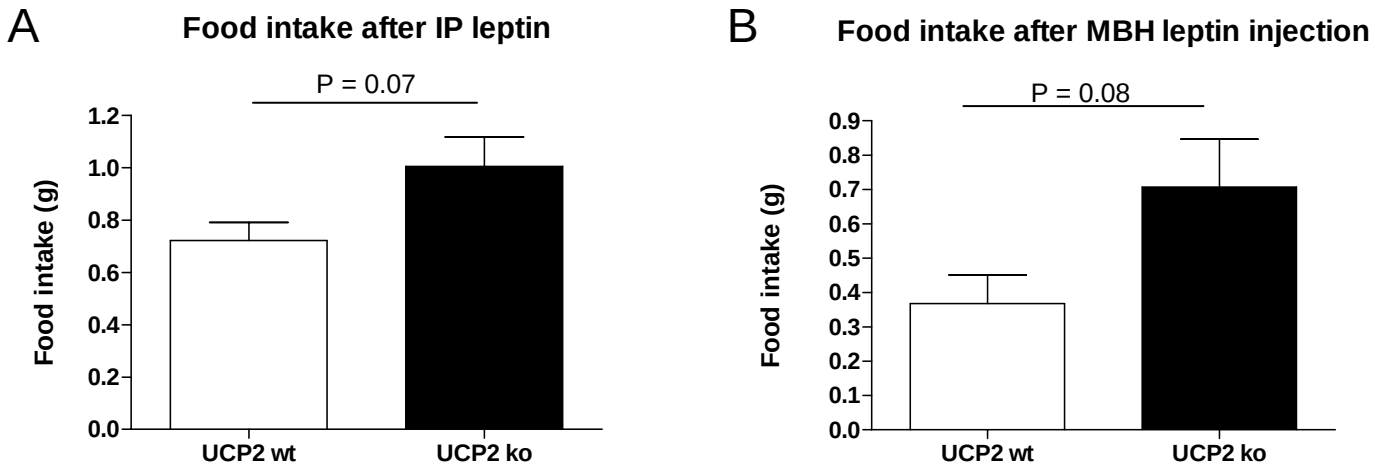

Suppl. Fig. 6

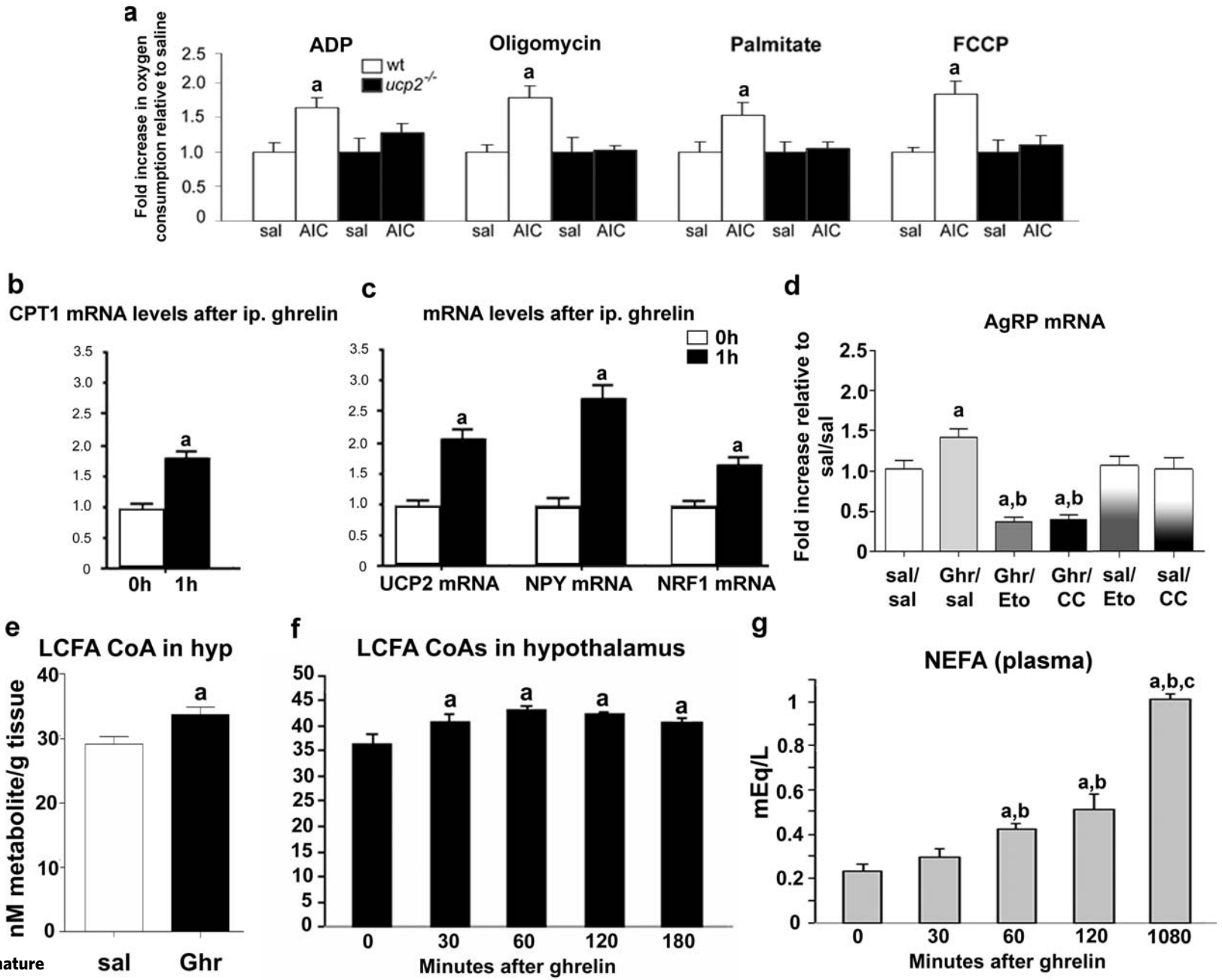
a
Fold increase in oxygen consumption relative to saline
ADP
Oligomycin
Palmitate
FCCP
wt
ucp2-/-
sal AIC sal AIC
b
CPT1 mRNA levels after ip. ghrelin
0h 1h
c
mRNA levels after ip. ghrelin
0h
1h
UCP2 mRNA
NPY mRNA
NRF1 mRNA
d
AgRP mRNA
Fold increase relative to sal/sal
sal/ sal
Ghr/ sal
Ghr/ Eto
Ghr/ CC
sal/ Eto
sal/ CC
e
LCFA CoA in hyp
nM metabolite/g tissue
sal
Ghr
f
LCFA CoAs in hypothalamus
Minutes after ghrelin
g
NEFA (plasma)
mEq/L
Minutes after ghrelin

Suppl. Fig. 7

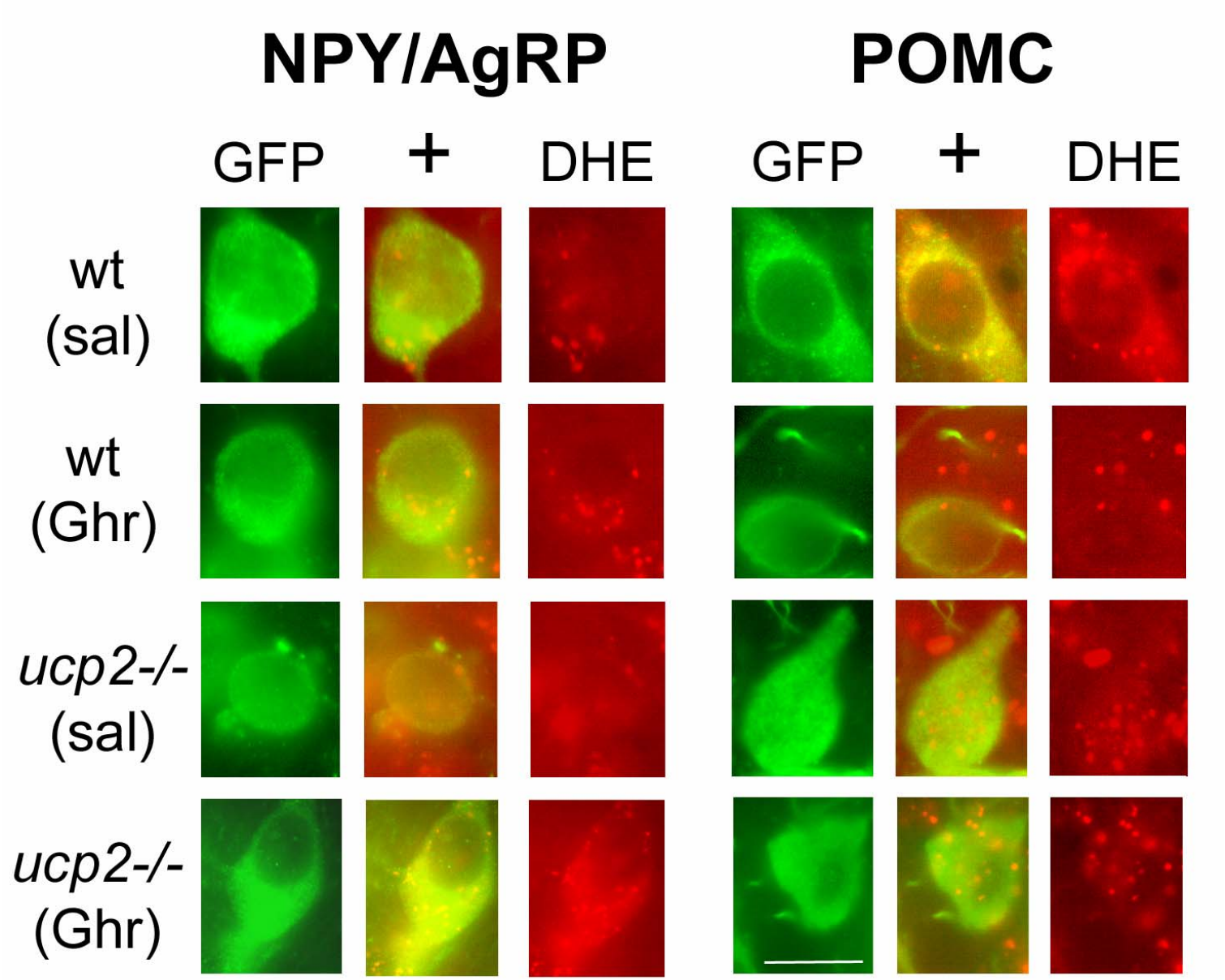

Suppl. Fig. 8

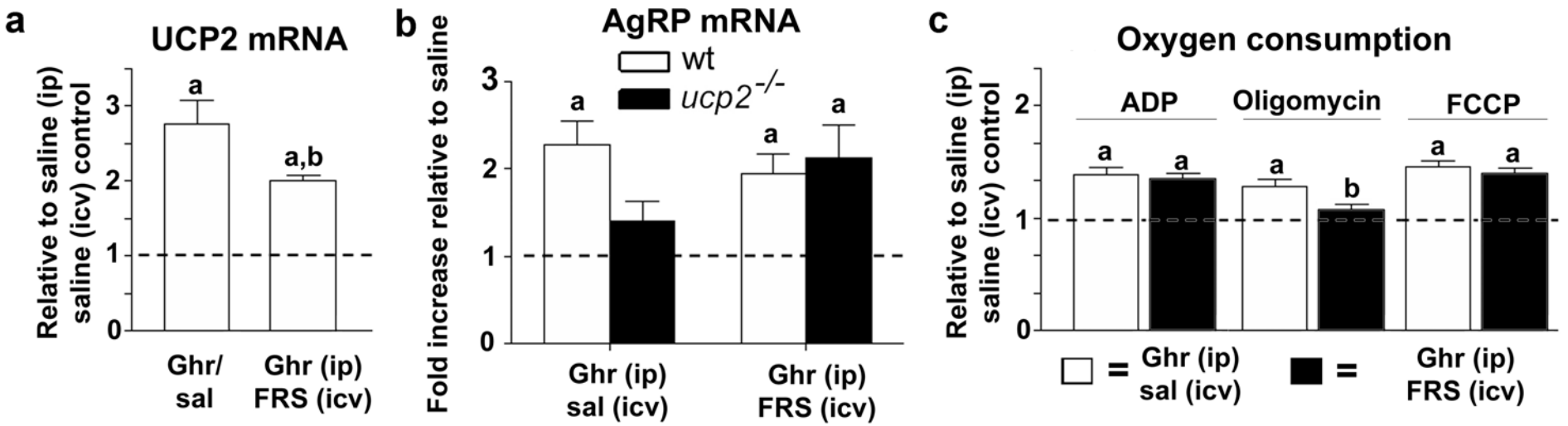
a
UCP2 mRNA
Relative to saline (ip)
saline (icv) control
a
a,b
Ghr/
sal
Ghr (ip)
FRS (icv)
b
AgRP mRNA
wt
ucp2-/-
Fold increase relative to saline
a
a
a
a
Ghr (ip)
sal (icv)
Ghr (ip)
FRS (icv)
c
Oxygen consumption
ADP
Oligomycin
FCCP
Relative to saline (ip)
saline (icv) control
a
a
a
b
a
a
= Ghr (ip)
sal (icv)
= Ghr (ip)
FRS (icv)

Suppl Fig. 9

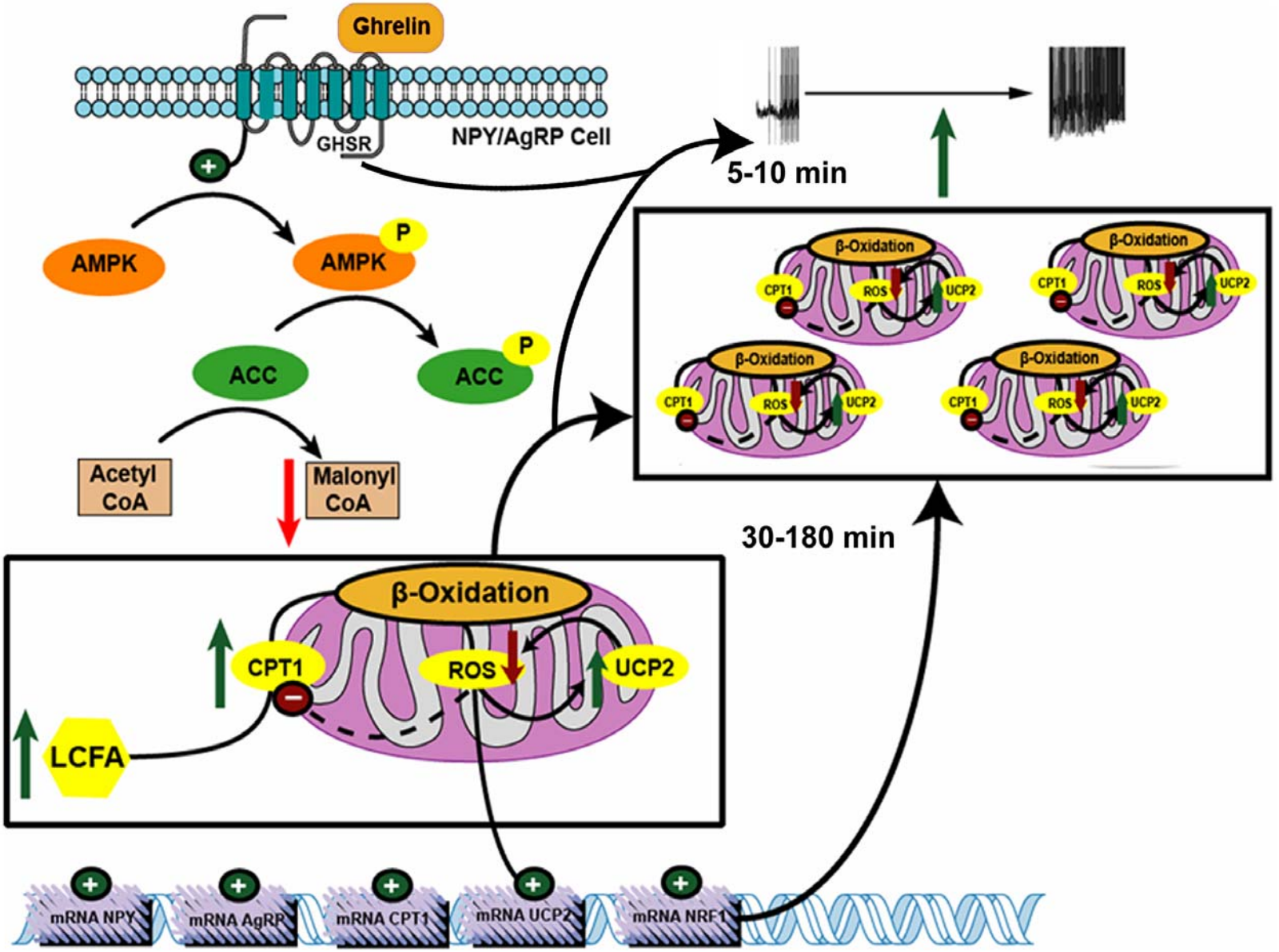
Ghrelin
GHSR
NPY/AgRP Cell
AMPK
AMPK
P
ACC
ACC
P
Acetyl CoA
Malonyl CoA
β-Oxidation
CPT1
ROS
UCP2
LCFA
5-10 min
30-180 min
mRNA NPY
mRNA AgRP
mRNA CPT1
mRNA UCP2
mRNA NRF1